Biogeosciences, 7, 859–867, 2010
www.biogeosciences.net/7/859/2010/

Biogeosciences

Ventilation of subterranean CO_2 and Eddy covariance incongruities over carbonate ecosystems

A. Were[1,2], P. Serrano-Ortiz[3,4], C. Moreno de Jong[5], L. Villagarcía[6], F. Domingo[2], and A. S. Kowalski[4]

[1]Dept. Hydrology and Geo-environmental Sciences, Vrije Universiteit Amsterdam, De Boelelaan 1085, 1081HV, Amsterdam, The Netherlands
[2]Dept. Desertificación y Geo-ecología, Estación Experimental de Zonas Áridas-CSIC, Ctra. de Sacramento s/n, 04120, La Cañada de San Urbano, Almería, Spain
[3]Dept. Biology, Univeristy of Antwerpen, Universiteitsplein 1, 2610 Wilrijk, Belgium
[4]Dept. Física Aplicada, Universidad de Granada, Av. Fuentenueva s/n, 18071, Granada, Spain
[5]Dept. Electromagnetismo y Física de la materia, Universidad de Granada, Fuente Nueva s/n, 18071, Granada, Spain
[6]Dept. Sistemas Físicos, Químicos y Naturales, Universidad Pablo de Olavide, Ctra. Utrera km. 1, 41013, Sevilla, Spain

Received: 23 October 2009 – Published in Biogeosciences Discuss.: 24 November 2009
Revised: 11 February 2010 – Accepted: 25 February 2010 – Published: 3 March 2010

Abstract. Measurements of CO_2 fluxes with Eddy Covariance (EC) systems are ongoing over different ecosystems around the world, through different measuring networks, in order to assess the carbon balance of these ecosystems. In carbonate ecosystems, characterized by the presence of subterranean pores and cavities, ventilation of the CO_2 accumulated in these cavities and pores can act as an extra source of CO_2 exchange between the ecosystem and the atmosphere. In this work we analyse the effect of the subterranean heterogeneity of a carbonate ecosystem on measurements of CO_2 fluxes by comparing measurements from two EC systems with distinct footprints. Results showed that both EC systems agreed for measurements of evapotranspiration and of CO_2 in periods when respiratory and photosynthetic processes were dominant (biological periods), with a regression slope of 0.99 and 0.97, respectively. However, in periods when the main source of CO_2 comes from the ventilation of subterranean pores and cavities (abiotic periods) agreement is not good, with a regression slope of 0.6. Ground-penetrating radar measurements of the sub-surface confirmed the existence of high sub-surface heterogeneity that, combined with different footprints, lead to differences in the measurements of the two EC systems. These results show that measurements of CO_2 fluxes with Eddy covariance systems over carbonate ecosystems must be taken carefully, as they may not be representative of the ecosystem under consideration.

Correspondence to: A. Were
(aeduar@falw.vu.nl)

1 Introduction

The importance of characterising the global carbon cycle is clear, since CO_2 is the principal greenhouse gas after water vapour (Schimel, 1995). In this context, accurate measurements of net carbon exchange between terrestrial ecosystems and the atmosphere are very important as terrestrial ecosystems are the main driver of global interannual variability in atmospheric CO_2 (Friend et al., 2007). The Eddy Covariance technique produces a direct measure of CO_2 exchange between the atmosphere and terrestrial ecosystems, and is therefore an indispensable tool to assess carbon ecosystem exchange (Matross et al., 2006; Baldocchi, 2003).

The net CO_2 flux between the terrestrial surface and the atmosphere has generally been interpreted as a biological flux due to photosynthetic and respiratory processes. However, over carbonate substrates, recent works highlight the role of geochemical rock weathering (dissolution and precipitation) processes in the total surface-atmosphere CO_2 exchange (e.g., Emmerich, 2003; Mielnick et al., 2005; Kowalski et al., 2008; Serrano-Ortiz et al., 2009). After rain events, infiltrating water dissolves the soil CO_2, acting as a CO_2 sink by reducing the CO_2 emissions, and percolates downward. The CO_2-enriched water seeping through fissures of bedrock creates new pores, fissures and even macropores (cavities) that characterise karstic systems. Therefore, pores, fissures and cavities near the surface can accumulate high concentrations of soil-derived CO_2 (Bourges et al., 2001; Wood, 1985) that can be isolated from soil-atmosphere exchange flows. Later, through the venting of these subterranean spaces, the

Published by Copernicus Publications on behalf of the European Geosciences Union.

gaseous CO_2 stored can be exchanged with the atmosphere (Weisbrod et al., 2009; Benavente et al., 2010). Therefore, the ventilation of cavities and fissures in carbonate ecosystems can yield an abiotic (in the sense that it is not directly produced by a biological process, like photosynthesis or respiration) source of CO_2 affecting the net ecosystem exchange (NEE), that under certain conditions can be as important as the biological processes traditionally considered (Kowalski et al., 2008; Serrano-Ortiz et al., 2009).

Measurements of net ecosystem exchange with the Eddy Covariance (EC) technique require sufficient fetch, meaning that the underlying surface extends homogeneously upwind for an extended distance (Baldocchi, 2003). This is a requirement met by nearly all EC used in different measuring networks around the world, such as FLUXNET (Baldocchi et al., 2001). However, when the flux has not only superficial, but also a subterranean source, as happens with the CO_2 coming from the venting of pores and cavities, then the subterranean heterogeneity can affect the fetch requirements of the EC measurements. According to this, in carbonate ecosystems it is important to analyse the reliability of EC measurements, as the presence of a subterranean source of CO_2, with a high spatial and temporal heterogeneity, can lead to net ecosystem exchange measurements that are not representative of the whole ecosystem. Moreover, the role of carbonate ecosystems in the global carbon balance is highlighted by the fact that carbonate substrates outcrop on ca. 12–18% of the water-free Earth (Ford and Williams, 1989).

In order to analyse the reliability of EC measurements in carbonate substrates, in this work we compared the measured fluxes of a carbonate ecosystem from two EC systems with distinct footprints. We differentiated between periods where photosynthesis and respiration were the main processes affecting the NEE (biological periods), versus those where the ventilation of subterranean pores and caves (abiotic periods) was the main process occurring (Serrano-Ortiz et al., 2009). We also compared the evapotranspiration flux from the two EC systems, as transpiration and evaporation are processes that are not strongly affected by subterranean heterogeneity. We expect that when the ecosystem fluxes are only dependent on the surface heterogeneity (as is the case of evapotranspiration and CO_2 fluxes caused by photosynthesis and respiration) both EC systems measure similarly. However, when abiotic CO_2 fluxes predominate, subsurface heterogeneity will yield differences between the CO_2 fluxes measured by the EC systems. Measurements of Ground penetrating radar (GPR) were also made to confirm the subterranean spatial heterogeneity of the carbonate ecosystem.

2 Material and method

2.1 Site description

The carbonate ecosystem studied in this work was located in the instrumented area of "El Llano de los Juanes", a sub-humid Mediterranean shrubland plateau located in the Sierra de Gador (Almeria, Southeast Spain; 36°55′41.7″ N; 2°45′1.7″ W), at 1600 m altitude and 25 km from the coast. The Sierra de Gádor consists of Triassic carbonate rocks (Vallejos et al., 1997), while in "El Llano de los Juanes" these carbonate rocks are mainly dark limestone, with 98±2% calcite (X-ray diffraction analysis). In this ecosystem, bare soil, gravel and rock represent 49.1% of the ground cover. Vegetation is sparse, with predominance (as % of ground cover) of three perennial species, *Festuca scariosa* (lag.) *Hackel* (18.8%), *Hormathophilla spinosa* (L.) *Kupfer* (6.8%) and *Genista pumila* (Vierh) ssp. *pumila* (5.5%). The extent of fetch is several hundreds of meters from the EC tower in every direction. More detailed site information can be found in Serrano-Ortiz et al. (2007).

2.2 Eddy covariance and micrometeorological measurements

Measurements of CO_2 flux (F_c), evapotranspiration (also referred to as latent heat flux, *LE*) and sensible heat flux (H) were carried out using two Eddy Covariance Systems (EC_1 and EC_2) installed on two towers with a 10 m separation (Fig. 1). Each system consisted of a three-axis sonic anemometer (CSAT-3, Campbell Scientific Inc., Logan, UT, USA; hereafter CSI) for measuring windspeed (3D) and sonic temperature, and an open-path infrared gas analyser (LI-COR 7500, Lincoln, NE, USA) for measuring CO_2 and water vapour densities. Measurements were recorded at 10 Hz by a data logger (CR23X, CSI) that calculated and stored means, variances and co-variances every 15 min. Eddy fluxes calculated from density covariances (Webb et al., 1980) and two coordinate rotations (McMillen, 1988) were carried out in post-processing, as well as the conversion to half-hour means following Reynolds' rules (Moncrieff et al., 1997). Measurements of CO_2 fluxes and *LE* with friction velocity lower than 0.2 m s^{-1} were eliminated from the analysis to avoid possible underestimation due to low turbulence (Serrano-Ortiz et al., 2009).

The two systems, EC_1 and EC_2, were installed in 2007 from late July to mid-October on towers separated by 10 m, and at heights of 2.75 m and 3.4 m, respectively. This height ensured that measurements were representative of the ecosystem's surface. Previously, to ensure that there were no significant differences between EC_1 and EC_2 due to instrument errors, both systems were installed on the same tower during 12 days, at a height of 2.80 m. The comparison between the data of the two EC systems was done considering

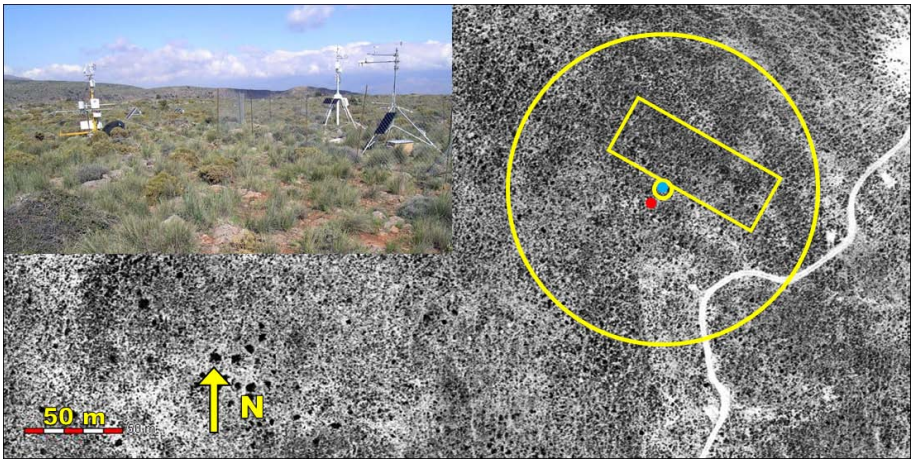

Fig. 1. Ortoimage of the measuring site, and the position of the two EC (EC_1: red point; EC_2: blue point). The rectangular area measured with the GPR, and the boundaries of the source area of EC_2 obtained with the footprint analysis (see Fig. 5 – unstable conditions) are shown. A picture of the site where both EC can be seen is shown on the upper left corner of the figure.

only daytime data, to avoid uncertainties due to the erratic behaviour of night-time turbulent fluxes.

In addition, soil water content (SWC) was measured with a water content reflectometer (CS615, CSI) and precipitation was quantified with a tipping bucket (0.2 mm) rain gauge (model 785 M, Davis Instruments Corp., Hayward, CA, USA). These measurements were made every 10 s, and stored every 15 min in the CR23X data-logger.

2.3 Footprint analysis

A footprint analysis was carried out tocompare the source areas of the two EC systems, both when EC_1 and EC_2 were installed in the same tower and when they were in separate towers. The Flux Source Area Model (FSAM) of Schmid (1994, 1997), widely used as a tool for estimating the source area of Eddy covariance measurements (e.g., Goeckede et al., 2004; Scott et al., 2003; Baldocchi et al., 2001) was selected. The FSAM model calculates the footprint function in the horizontal plane, calculating the minimum area responsible for a given % of the total source weight. According to the footprint function, there is a source point that has the maximum relative source weight of all the source area of the sensor (referred to as the point of maximum source weight) and from this point the source weight of the source area falls towards all directions (Schmid, 1994, 2002). We have considered the dimensions of the source area responsible for the 50% of the total source weight (hereafter referred to as 50% source area) calculated with FSAM. This source area includes the point of maximum source weight, and according to Schmid (1997) a flux source point located on or outside the 50% source area boundaries would have to be from 5 to 10 times stronger than the point of maximum source weight, in order to achieve a similar response on the EC sensors. Therefore, we considered that the 50% source areas were appropriate to compare the flux source areas of both EC systems.

The FSAM model calculates the dimensions of the source area of a given sensor as a function of the height of the sensor, the atmospheric stability conditions and the lateral wind speed fluctuations. In this context, three dimensionless ratios are used: $(z_r-d)/z_0$, $(z_r-d)/L$ and σ_v/u_*, where z_r is the height of the EC tower, d the displacement height, L the Obukhov length, σ_v the standard deviation of cross-wind velocity fluctuations, z_0 the roughness length, and u_* the friction velocity. While $(z_r-d)/z_0$ is constant for the same z_r and σ_v/u_* is very stable, the stability factor $(z_r-d)/L$ has a range of values according to the atmospheric conditions that determine the dimensions of the resulting source areas. Therefore, $(z_r-d)/L$ and σ_v/u_* were calculated for each half hour, and separated in two groups: data with unstable atmospheric conditions ($(z_r-d)/L<-0.01$) and data with near neutral atmospheric conditions ($-0.01(z_r-d)/L<0.01$) (ranges taken from Monteith and Unsworth, 1990). Notice that there were no data with stable conditions, as stable conditions occur at night, whereas only daytime data were considered. The FSAM model calculates the dimensions of the source area, by calculating the distance from the sensor of the near-end and far-end boundaries of the source area. At a given wind direction, the dimensions of the source area vary with the atmospheric stability conditions. Thus, as the stability conditions get more unstable (corresponding to smaller values of $(z_r-d)/L$), the dimension of the source area decreases, and it gets closer to the sensor, meaning that both the near- and far-end boundaries of the source area get closer to the sensor. The opposite occurs when the conditions get more stable (higher values of $(z_r-d)/L$).

Table 1. Values of parameters used to run the FSAM model. FSAM was run for the period when EC_1 and EC_2 were installed in the same tower, and when they were installed in separate towers. Runs 1, 2, 5 and 6 used the minimum and maximum $(z_r - d)/L$ obtained during unstable conditions, and runs 3, 4, 7 and 8 used the minimum and maximum $(z_r - d)$/L obtained during neutral conditions.

	Atmospheric conditions	runs	EC_1 $\frac{(z_r-d)}{L}$	EC_1 $\frac{(z_r-d)}{z_0}$	EC_1 $\frac{\sigma_v}{u_*}$	EC_2 $\frac{(z_r-d)}{L}$	EC_2 $\frac{(z_r-d)}{z_0}$	EC_2 $\frac{\sigma_v}{u_*}$
Same tower	Unstable	1	−0.104	38.9	3.26	−0.105	38.9	3.03
		2	−0.011	38.9	3.26	−0.01	38.9	3.03
	Neutral	3	−0.01	38.9	4.33	−0.009	38.9	4.3
		4	0.0005	38.9	4.33	0.0006	38.9	4.3
Separate towers	Unstable	5	−0.9	37.5	3.6	−0.98	47.5	3.66
		6	−0.01	37.5	3.6	−0.01	47.5	3.66
	Neutral	7	−0.01	37.5	4.19	−0.01	47.5	4.74
		8	0.003	37.5	4.19	0.003	47.5	4.74

Therefore, in order to obtain the maximum and minimum dimensions of the 50% source areas, we ran the FSAM model using the maximum and minimum values of $(z_r - d)/L$, and an averaged σ_v/u_*, for each range of stability conditions. This was done both for the period when EC_1 and EC_2 were on the same tower, and for the period when they were in separate towers. Table 1 summarizes the values of the parameters used to run FSAM.

The values of z_0 and d were calculated from the relations with the average plant height of the ecosystem ($h = 0.5$ m), as proposed by Shuttleworth and Gurney (1990).

2.4 GPR measurements

In order to investigate the presence and location of caves and pores in the subsurface of the footprint area of the two EC systems, measurements were made with a GPR (Ground-penetrating radar) system in a 80 m × 30 m area to the North-east of the towers (Fig. 1). This area included the maximum source weighted points (according to the footprint analysis mentioned before) for both EC systems, for the main wind directions coming from the North to East directions.

Seven profiles, 80 m long and with 5 m separation, were measured using a GPR proEX (Malå, Sweden) equipped with a shielded antenna of 250 MHz central frequency, applying time windows of 200 ns, 5 cm measurement steps, a sampling frequency of 1551 MHz, and 898 samples per scan. For the soil type of the measured site, i.e. limestone, the average speed is 0.1 m/ns, this being the value used for all the profiles carried out in reflection mode. According to the average speed and the recording time window, the depth of investigation was between 5 and 8 m.

2.5 Comparison of flux measurements between EC systems

To assess the agreement of the fluxes measured by EC_1 and EC_2 we used different methods. Firstly, we calculated the linear regression between the fluxes measured by EC_1 and EC_2. To verify how significantly different from one and zero were the slopes and y-intercepts obtained from the linear regressions, as a measure of the difference between both EC system measurements, we performed two statistical analysis. On one hand, we used a t-test to check if there were significant differences between the linear regression and a linear model where the y-intercept was set to 0. On the other hand, we used an ANOVA test to check if there were significant differences between the linear regression and a linear model where the slope was set to 1. Significant results (p-value$<$0.05) would indicate that the y-intercept is significantly different from 0, or the slope is significantly different from 1, and a non significant result (p-value$>$0.5) would indicate that for the data used we can assume that the y-intercept is not significantly different from 0, and the slope is not significantly different from 1. This statistical analysis was made with the R programme (R development core team, 2008).

On the other hand, we calculated the root mean square difference (ε) as:

$$\varepsilon = \sqrt{\frac{1}{n}\sum_{i=1}^{n}\left(F_{1,i} - F_{2,i}\right)^2} \quad (1)$$

where $F_{1,i}$ and $F_{2,i}$ are the ith fluxes (either F_c or LE) measured by EC_1 and EC_2, respectively. As the units of ε are different for F_c and LE, to have a notion of the magnitude of the ε and be able to compare them, we calculated the relative root mean square difference (ε_r) relating this parameter to the average of the fluxes measured by both EC systems, as follows:

$$\varepsilon_r = \left[\varepsilon \Big/ \left(\frac{\overline{F_1} + \overline{F_2}}{2}\right)\right] \cdot 100 \quad (2)$$

For the case of F_c, the average does not give a notion of the magnitude in $\mu mol\, m^{-2}\, s^{-1}$ of the F_c data, due to the

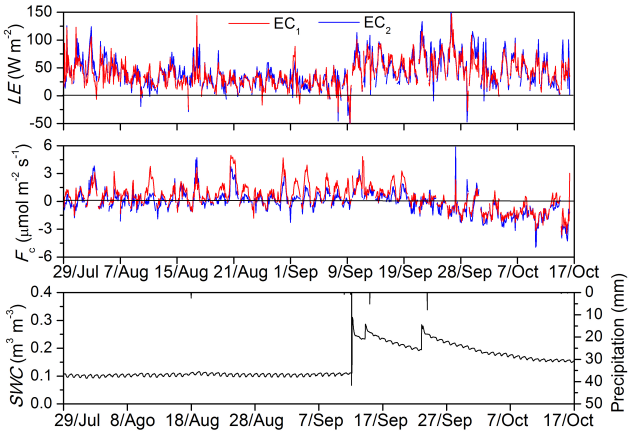

Fig. 2. Values of diurnal *LE* and F_c measured every 30 min by EC_1 and EC_2 for the period from end of July to mid October, when both systems were located on two separate towers. Soil Water Content (SWC) and precipitation are also represented. Notice that *LE* and F_c are diurnal data (no night-time data are shown) from non-continuous days – as no gap-filling was used – while SWC and precipitation are continuous data for the whole period.

presence of positive and negative values. To avoid this effect, $\overline{F_1}$ and $\overline{F_2}$ were calculated with the absolute values of F_c. In the case of *LE*, $\overline{F_1}$ and $\overline{F_2}$ were calculated as a normal average, due to the absence of negative *LE* values, as only daytime data were considered.

Comparison of fluxes from EC_1 and EC_2 was done for the whole period studied. However, as mentioned in the Introduction, another comparison between F_c fluxes was done, differentiating between biological and abiotic periods. Following Serrano-Ortiz et al. (2009) we considered biological periods with SWC > 15% and Bowen ratio (H/LE) lower than 4, and abiotic periods with SWC<15% and Bowen ratio higher than 4.

3 Results

For the period where both EC systems were on separate towers, the values of *LE* measured ranged between ca. 160 W m^{-2} and −60 W m^{-2}, while F_c ranged between ca. 6 µmol m^{-2} s^{-1} and −5 µmol m^{-2} s^{-1} (Fig. 2). The values of SWC and precipitation (Fig. 2) showed that before 12 September the SWC was very constant (around 10% vol.) but after the important precipitation event on that day (more than 40 mm), SWC reached 30%, and remained above 15%. This change in SWC is reflected in higher values of *LE*, and the beginning of a transition in F_c from positive (CO_2 release) to negative (CO_2 uptake). According to the criteria for separating between biological and abiotic periods mentioned in the previous section, the abiotic period lasted from 29 July until the first rain event on 12 September, when the biological period is considered to have begun (Fig. 2).

For the period where EC_1 and EC_2 were on the same tower, both systems showed good agreement for F_c ($F_{c2} = 1.05\,F_{c1} + 0.08$, $R^2 = 0.97$; $\varepsilon = 0.32$ µmol m^{-2} s^{-1}), and fair agreement for *LE* ($LE_2 = 0.87\,LE_1 + 1.98$, $R^2 = 0.93$; $\varepsilon = 7.28$ W m^{-2}).

Figure 3 shows the linear regressions for *LE* and F_c between the two EC systems installed on separate towers. These results show that the agreement between EC_1 and EC_2 was better for *LE* (slope = 0.99) than for F_c (slope = 0.82) (Table 2). Moreover, results showed that the slope of the regression for *LE* was not significantly different from 1, whereas for F_c the slope was significantly different from 1 (Table 2), showing that the agreement between EC_1 and EC_2 fro *LE* was much higher than for F_c. The ε_r for *LE* was 32.3%, while the ε_r for F_c was up to 81.5%.

Figure 4 represents the linear regressions between F_{c1} and F_{c2} for the biological and abiotic periods. Results showed clearly better agreement for the biological period than for the abiotic period, where the slope of the regression for the biological period was not significantly different from 1, whereas for the abiotic period it was significantly different from 1 (Table 2). For the biological period the y-intercept was significantly different from 0, however its magnitude was small (0.3 µmol m^{-2} s^{-1}, Table 2). Moreover, the ε for the abiotic period was 15.4% higher than the ε for the whole dataset, while the ε for the biological period was 21.7% lower than the ε for the whole dataset (Table 2).

Figure 5 represents the minimum near-end (smaller circles around the sensor) and maximum far-end (larger circles around the sensor) of the 50% source areas calculated with FSAM for each EC system mounted in separate towers, both for the data with unstable conditions and for the data with near neutral conditions. Therefore, the area comprised within both circles is the area that includes all the 50% source areas of each EC system for every wind direction and stability condition found during the period studied. Also represented are the wind directions separated into intervals of 45°. Unstable conditions represented more than 75% of all data, and for these data the dominant winds came from between the North and East directions (60%). The far-end source area boundaries for these wind directions differed by up to 30 m. For neutral conditions, representing less than 25% of the data, the main wind direction was from the South (33% of the data), and as can be seen in Fig. 5, the far-end source area boundaries for that wind direction differed by less than 9 m.

An analysis of the data from the biological and abiotic periods separately, showed that during the biological period 86.3% of the data corresponded to unstable atmospheric conditions, and 53.9% of the wind directions came from the North to East directions, and 23% came from the South. In the case of the abiotic period, 95% of the data corresponded to unstable atmospheric conditions, and 76% of the wind directions came from the North to East directions, and 15% came from the South. Therefore, for both periods more than 50% of the wind directions came from the North to East

Table 2. Parameters of the linear regressions (slope and y-intercept), coefficient of determination (R^2), the root mean square error (ε) and the relative root mean square error (ε_r) obtained by comparing F_c and LE measured with EC_1 and EC_2. Y-intercept and ε values for F_c and LE are in µmol m^{-2} s^{-1} and W m^{-2}, respectively. Parameters were obtained for the total set of data ($n = 665$), and for the biological ($n = 248$) and abiotic periods ($n = 252$), separately. Significance codes, from least to most significant, indicate: "n.s." (not significant) $p > 0.5$; "*" $0.05 > p > 0.01$; "**" $0.01 > p > 0.001$; "***" $p < 0.001$.

		slope	y-intercept	R^2	ε	ε_r (%)
Total data	LE	$0.99^{n.s.}$	2.5^{*}	0.71^{***}	14.23	32.3
	F_c	0.82^{***}	-0.39^{***}	0.76^{***}	0.82	81.5
Biological period	F_c	$0.97^{n.s.}$	-0.3^{***}	0.81^{***}	0.64	61.3
Abiotic period	F_c	0.60^{***}	-0.26^{***}	0.73^{***}	0.95	102.6

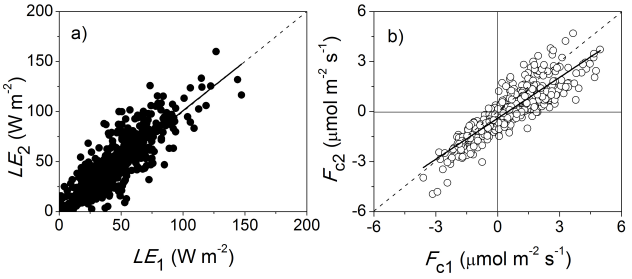

Fig. 3. Linear regressions between LE **(a)** and F_c **(b)** measured with EC_1 (x axis) and EC_2 (y axis) for the period where they were on separate towers. The regression line (solid line) and the 1:1 line (discontinuous line) are shown.

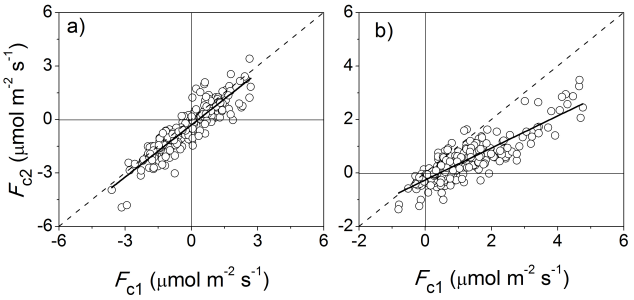

Fig. 4. Linear regressions between F_c measured with EC_1 (x axis) and EC_2 (y axis), for the biological period **(a)** and abiotic period **(b)**. The regression line (solid line) and the 1:1 line (discontinuous line) are shown.

directions, where the higher differences between the footprint of both EC_1 and EC_2 are observed (Fig. 5, unstable conditions).

As expected, for the period when both EC systems were mounted on the same tower, the boundaries of the source areas of both EC systems were the same, with differences of less than 1 m (data not shown). Therefore, the footprint analysis showed that for certain wind directions, the source areas of the two EC systems mounted in separate towers were different (Fig. 5).

Figure 6 represents the radargramme of one of the seven profiles done with a GPR to survey the subsurface for the possible presence of cavities and fractures. As already indicated, the profiles were done along an 80 m per 30 m area at the North-east of the towers (Fig. 1). According to the above source area analysis, the area measured with the GPR was located within the boundaries of the source areas of both towers, for at least 45% of the total data. The radargrammes showed three distinctive zones: i) a shallow zone with a thickness between 0–2 m, marked by multiple reflections and limited by a bedding plane (labelled B in Fig. 6) – this region is characterised by strong vertical fracturing and cracks; ii) a deeper zone below, where the absence of strong reflections could be caused by the homogeneity of the material (A in Fig. 6) or due to the attenuation of the signal; and

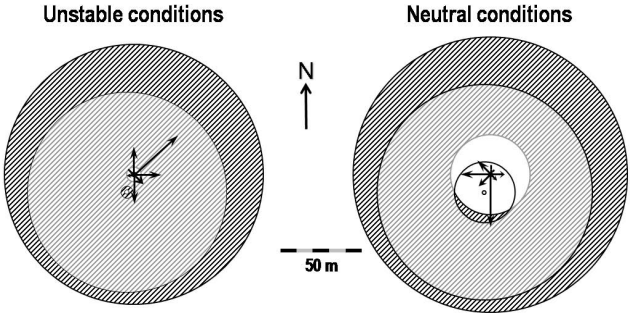

Fig. 5. Schematic representation of the area comprised between the near-end and far-end boundaries of the 50% source areas calculated with FSAM for EC_1 (light white) and EC_2 (black stripes), mounted on separate towers, and for unstable atmospheric conditions and near-neutral atmospheric conditions. The arrows indicate the direction from where the wind is coming, separated in 45° angles, being the length of the arrow the proportion of the total data coming from that specific 45° wind direction.

iii) a possible cavity between two bedding planes (labelled C in Fig. 6). Although a more thorough survey should be done to determine the exact location of fractures and cavities, these results reveal the existence of discontinuities of the rock, bedding planes and fractures in the subsurface of the measured area.

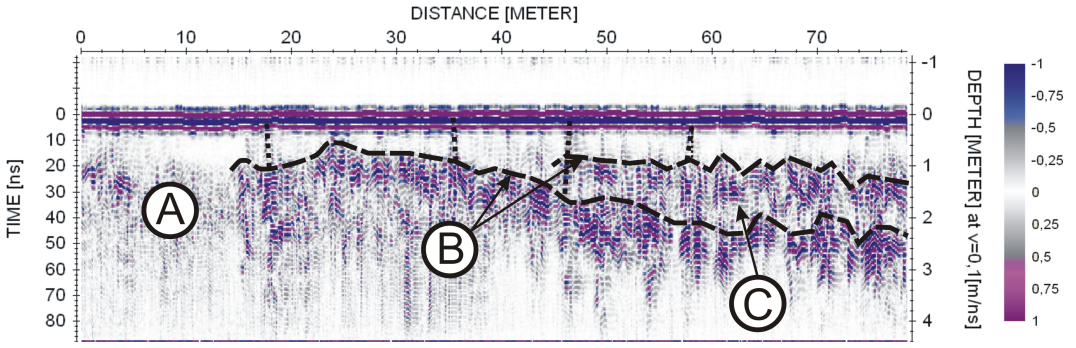

Fig. 6. Radargramme of one of the seven 80 m profiles carried out with a GPR, to the Northeast of the EC towers (location of the area surveyed with the GPR is shown in Fig. 1). A: massive and compact limestones, B: bedding plane, C: possible cavity. Vertical dotted lines indicate fractures and cracks.

4 Discussion and conclusions

Measurement of turbulent fluxes with Eddy covariance systems requires a sufficient fetch to generate an internal boundary layer where fluxes are constant with height (Kaimal and Finnigan, 1994). To match this requirement, Eddy covariance systems are mounted on towers at a height within this boundary layer, and in areas with uniform vegetation, with no strong discontinuities that can affect the EC measurements in a way that they no longer are representative of the whole area. However, this has worked when measuring fluxes from scalars (CO_2, water vapour or temperature) whose main sources come from the surface, either soil surface or vegetation.

The CO_2 is a gas with an important effect in the atmosphere as a greenhouse gas, hence the importance of studying the accurate exchange flux of this gas between the surface and the atmosphere. Moreover, CO_2 is a key molecule in the carbon cycle of ecosystems, due to the photosynthesis and respiration processes taking place at vegetation and soil levels. In this work, we address the importance of the CO_2 stored in the pores and cavities of the sub-surface of carbonate ecosystems in the net exchange of CO_2 between the surface and the atmosphere.

Recent works have shown evidence of the existence of a subterranean source of CO_2 coming from the ventilation of pores and cavities located in the sub-surface of carbonate ecosystems (Kowalski et al., 2008; Emmerich, 2003; Baldini et al., 2006). Moreover, Weisbrod et al. (2008) have demonstrated the existence of a convective exchange mechanism between fractures and atmosphere in an arid area with a high level of porosity in the soil. In the same carbonate area considered in this paper, Kowalski et al. (2008) indicated that this sub-surface source of CO_2 is stronger during dry periods when the low soil water content enhances this leakage of sub-surface CO_2 through the soil pores. This so called abiotic source of CO_2 can be predominant during dry periods, when the biological processes occurring on the surface are limited, vegetation is considered to be senescent, and heterotrophic respiration can be neglected (Eliasson et al., 2005; Serrano-Ortiz et al., 2009).

According to these considerations, in this paper we present evidence of the effect of the spatial heterogeneity of the CO_2 sub-surface abiotic source on the Eddy covariance (EC) system CO_2 flux measurements on a carbonate area. At first, we compared the measured evapotranspriation (LE) and CO_2 flux (F_c) of two separate EC towers (EC_1 and EC_2). We have considered LE as a control value to compare with F_c, because LE originates at the surface of the ecosystem, through the evaporation of the soil and vegetation surface, and the transpiration of vegetation. Results show that the agreement between EC_1 and EC_2 is better for LE, than for F_c (Fig. 3 and Table 2). Secondly, we compared F_c from the two EC in periods with predominance of biological surface processes (biological periods), with higher SWC that favour photosynthesis and respiration, and in periods with predominance of ventilation sub-surface processes and low biological activity (abiotic periods). We observed that the agreement between both systems was very good in the biological period (Fig. 4 and Table 2), whereas in the abiotic period there was a clear disagreement between the two EC systems (slope = 0.6 and $\varepsilon = 0.95\,\mu mol\,m^{-2}\,s^{-1}$, in Table 2). The presence of positive F_c data in the biological period, indicating release of CO_2, can be due to high respiration rates after a rain event (Schwinning and Sala, 2004). This disagreement during abiotic periods can be explained by the spatial heterogeneity of the pores and fractures through which CO_2 outflows. The analysis of the footprint of the two EC systems shows that for the main wind directions, the source areas of the two EC systems located in separate towers are different (Fig. 5). Hence, if the source area of one of the EC includes an outflow of CO_2, this tower will measure a different amount of CO_2 flux than the other tower during the abiotic period. Although for the biological period there is a fairly higher percentage of data with wind directions from the South, where the difference between the footprints of EC_1 and EC_2 are lower

(Fig. 5), compared to the abiotic period (23% and 15%, respectively), we think that this is not enough to explain the clear difference in the agreement of both EC systems observed for the biological and abiotic periods.

To reinforce the idea of the heterogeneity of the subsurface of the ecosystem to explain the disagreement between the EC systems, radar measurements confirm the presence of fractures and cavities in the subsurface, whose distribution is not uniform (Fig. 6). Moreover, the gaseous CO_2 stored in a certain cavity or pore in the soil can outflow from a point located at a distance from where it originated. Therefore, not only the spatial heterogeneity of the carbonate subterranean porespace, but especially of the outflow points, must be taken into account when measuring the surface-atmosphere CO_2 exchange in carbonate areas.

Though efforts have been made to use an EC system to locate and quantify surface CO_2 outflows (Lewicki et al., 2009), results were not conclusive. Therefore, measurements of CO_2 fluxes with EC towers over carbonate ecosystems must be interpreted with care, as they may not be representative of the whole area, since these ecosystems have additional sources of CO_2 due to ventilation processes across fissures, pores and cavities. Thus, in these ecosystems with a high subsurface heterogeneity, the carbon balance measured only with Eddy covariance measurements should be corroborated with additional techniques.

Acknowledgements. This work was partly funded by: EU-FP7 (grant 205294); the Spanish Science Ministry projects PROBASE (CGL2006-11619/HID), CARBORED-ES (CGL2006-14195-C02-01/CLI), $TEC_2$007-66698-C04-02, CSD2008-00068, DEX-530000-2008-105 and TIC1541; and by the regional government of Andalusia through the projects BACAEMÁ (RNM-332), AQUASEM (P06-RNM-01732) and GEOCARBO (RNM-3721). AW and PSO are funded by a post-doctoral fellowship from the Ministry of Science and Innovation. LV benefited from a 6 months stay at the VUA (Amsterdam, Netherlands) funded by the regional government of Andalusia. The authors would like to thank Alfredo Durán for his help in the field.

Edited by: G. Wohlfahrt

References

Baldini, J. U. L., Baldini, L. M., McDermott, F., and Clipson, N.: Carbon dioxide sources, sinks, and spatial variability in shallow temperate zone caves: Evidence from Ballynamintra cave, Ireland, J. C. Karst Stud., 68(1), 4–11, 2006.

Baldocchi, D., Falge, E., Gu, L. H., Olson, R., Hollinger, D., Running, S., Anthoni, P., Bernhofer, C., Davis, K., Evans, R., Fuentes, J., Goldstein, A., Katul, G., Law, B., Lee, X. H., Malhi, Y., Meyers, T., Munger, W., Oechel, W., Paw U, K. T., Pilegaard, K., Schmid, H. P., Valentini, R., Verma, S., Vesala, T., Wilson, K., and Wofsy, S.: FLUXNET: A new tool to study the temporal and spatial variability of ecosystem-scale carbon dioxide, water vapor, and energy flux densities, B. Am. Meteorol. Soc., 82(11), 2415–2434, 2001.

Baldocchi, D.: Assessing the eddy covariance technique for evaluating carbon dioxide exchange rate of ecosystem: past, present and future, Glob. Change Biol., 9, 479–492, 2003.

Benavente, J., Vadillo, I., Carrasco, F., Soler, A., Liñán, C., and Moral, F.: Air Carbon Dioxide Contents in the Vadose Zone of a Mediterranean Karst, Vadose Zone J., 9, 126–136, 2010.

Bourges, F., Mangin, A., and d'Hulst, D.: Carbon dioxide in karst cavity atmosphere dynamics: the example of the Aven d'Orgnac (Ardeche), C. R. Acad. Sci. Paris, Sciences de la Terre et des planètes/Earth and Planetary Sciences, 333, 685–692, 2001.

Eliasson, P. E., McMurtrie, R. E., Pepper, D. A., Strömgren, M., Linder, S., and Agren, G. I.: The response of heterotrophic CO_2 flux to soil warming, Global Change Biol., 11(1), 167–181, 2005.

Emmerich, W. E.: Carbon dioxide fluxes in a semiarid environment with high carbonate soils, Agr. Forest Meteorol., 116(1–2), 91–102, 2003.

Ford, D. C. and Williams, P. W.: Karst Geomorphology and Hydrology, Unwin Hyman, London, 601 pp., 1989.

Friend, A. D., Arneth, A., Kiang, N. Y., Lomas, M., Ogee, J., Rodenbeckk, C., Running, S. W., Santaren, J. D., Sitch, S., Viovy, N., Woodward, F., and Zaehle, S.: FLUXNET and modelling the global carbon cycle, Glob. Change Biol., 13, 610–633, 2007.

Goeckede, M., Rebmann, C., and Foken, T.: A combination of quality assessment tools for eddy covariance measurements with footprint modelling for the caracterisation of complex sites, Agr. Forest Meteorol., 127(3–4), 175–188, 2004.

Kaimal, J. C. and Finnigan, J. J.: Atmospheric Boundary Layer Flows: Their Structure and Measurement, Oxford University Press, 289 pp., 1994.

Kowalski, A. S., Serrano-Ortiz, P., Janssens, I. A., Sánchez-Moral, S., Cuezva, S., Domingo, F., Were, A., and Alados-Arboledas, L.: Can flux tower research neglect geochemical CO_2 exchange?, Agr. Forest Meteorol., 148(6–7), 1045–1054, 2008.

Lewicki, J. L., Hilley, G. E., Fischer, M. L., Pan, L., Oldenburg, C. M., Dobeck, L., and Spangler, L.: Eddy covariance observations of surface leakage during shallow subsurface CO_2 releases, J. Geophys. Res., 114, D12302, doi:10.1029/2008JD011297, 2009.

Matross, D. M., Andrews, A., Pathmathevan, M., Gerbig, C., Lin, J. C., Wofsy, S. C., Daube, B. C., Gottlieb, E. W., Chow, V. Y., Lee, J. T., Zhao, C., Bakwin, P. S., Munger, J. W., and Hollinger, D. Y.: Estimating regional carbon exchange in New England and Quebec by combining atmospheric, ground-based and satellite data, Tellus B, 58(5), 344–358, 2006.

McMillen, R. T.: An eddy correlation technique with extended applicability to non-simple terrain, Bound.-Lay. Meteorol., 43, 231–245, 1988.

Mielnick, P., Dugas, W. A., Mitchell, K., and Havstad, K.: Long-term measurements of CO2 flux and evapotranspiration in a Chihuahuan desert grassland, J. Arid Environ., 60(3), 423–436, 2005.

Moncrieff, J. B., Massheder, J. M., Bruin, H., Elbers, J., Friborg, T., Heusinkveld, B., Kabat, P., Scott, S., Soegaard, H., and Verhoef, A.: A system to measure surface fluxes of momentum, sensible heat, water vapour and carbon dioxide, J. Hydrol., 188–189, 589–611, 1997.

Monteith, J. L. and Unsworth, M. H.: Principles of environmental physics, Hodder & Stoughton, London, 291 pp., 1990.

R Development Core Team: R: A language and environment for statistical computing, R Foundation for Statistical Computing,

Vienna, Austria, ISBN 3-900051-07-0, online available at: http://www.R-project.org, 2008.

Schimel, D. S.: Terrestrial ecosystems and the carbon cycle, Glob. Change Biol., 1(1), 77–91, 1995.

Schmid, H. P.: Source areas for scalars and scalar fluxes, Bound.-Lay. Meteorol., 67, 293–318, 1994.

Schmid, H. P.: Experimental design for flux measurements: matching scales of observations and fluxes, Agr. Forest Meteorol., 87, 179–200, 1997.

Schwinning, S. and Sala, O. E.: Hierarchy of responses to resource pulses in arid and semi-arid ecosystems, Oecologia, 141, 211–220, 2004.

Scott, R. L., Watts, C. J., Payan, J. G., Edward, E., Goodrich, D. C., Williams, D., and Shuttleworth, W. J.: The understory and overstory partitioning of energy and water fluxes in an open canopy, semiarid woodland, Agr. Forest Meteorol., 114, 127–139, 2003.

Serrano-Ortiz, P., Kowalski, A. S., Domingo, F., Rey, A., Pegoraro, E., Villagarcía, L., and Alados-Arboledas, L.: Variations in daytime net carbon and water exchange in a montane shrubland ecosystem in southeast Spain, Photosynthetica, 45(1), 30–35, 2007.

Serrano-Ortiz, P., Domingo, F., Cazorla, A., Were, A., Cuezva, S., Villagarcía, L., Alados-Arboledas, L., and Kowalski, A. S.: Interannual CO_2 exchange of a sparse Mediterranean shrubland on a carbonaceous substrate, J. Geophys. Res., 114, G04015, doi:10.1029/2009JG000983, 2009.

Shuttleworth, W. J. and Gurney, R. J.: The theoretical relationships between foliage temperature and canopy resistance in sparse crops, Q. J. Roy. Meteor. Soc, 116, 497–519, 1990.

Vallejos, A., Pulido-Bosch, A., Martin-Rosales, W. and Calvache, M. L.: Contribution of environmental isotopes to the understanding of complex hydrologic systems. A case study: Sierra de Gádor, SE Spain, Earth Surf. Proc. Land., 22, 1157–1168, 1997.

Webb, E. K., Pearman, G. I., and Leuning, R.: Correction of flux measurements for density effects due to heat and water vapour transfer, Q. J. Roy. Meteor. Soc., 106, 85–100, 1980.

Weisbrod, N., Dragila, M. I., Nachshon, U., and Pillersdorf, M.: Falling through the cracks: The role of fractures in Earth-atmosphere gas exchange, Geophys. Res. Lett., 36, L02401, doi:10.1029/2008GL036096, 2009.

Wood, W. W.: Origin of caves and other solution openings in the unsaturated (vadose) zone of carbonate rocks: A model for CO_2 generation, Geology, 13(11), 822–824, 1985.